

Article

A Pixel Circuit for Compensating Electrical Characteristics Variation and OLED Degradation

Ning Wei ^{1,2}, Hongzhen Chu ¹, Bo Yu ¹, Huicheng Zhao ¹, Yuehua Li ^{1,*}, Xinlin Wang ¹ and Hongyu He ^{1,2}¹ School of Electrical Engineering, University of South China, Hengyang 421001, China² School of Electronics and Information, Yangtze University, Jingzhou 434023, China

* Correspondence: nhliyuehua@usc.edu.cn; Tel.: +86-18607343306

Abstract: In recent years, the active-matrix organic light-emitting diode (AMOLED) displays have been greatly required. A voltage compensation pixel circuit based on an amorphous indium gallium zinc oxide thin-film transistor is presented for AMOLED displays. The circuit is composed of five transistors–two capacitors (5T2C) in combination with an *OLED*. In the circuit, the threshold voltages of both the transistor and the *OLED* are extracted simultaneously in the threshold voltage extraction stage, and the mobility-related discharge voltage is generated in the data input stage. The circuit not only can compensate the electrical characteristics variation, i.e., the threshold voltage variation and mobility variation, but also can compensate the *OLED* degradation. Furthermore, the circuit can prevent the *OLED* flicker, and can achieve the wide data voltage range. The circuit simulation results show that the *OLED* current error rates (CERs) are lower than 3.89% when the transistor’s threshold voltage variation is $\pm 0.5V$, lower than 3.49% when the mobility variation is $\pm 30\%$.

Keywords: pixel circuit; voltage programming; threshold voltage variation; mobility variation; *OLED* degradation



Citation: Wei, N.; Chu, H.; Yu, B.; Zhao, H.; Li, Y.; Wang, X.; He, H. A Pixel Circuit for Compensating Electrical Characteristics Variation and *OLED* Degradation.

Micromachines **2023**, *14*, 857. <https://doi.org/10.3390/mi14040857>

Academic Editor: Meng Zhang

Received: 8 March 2023

Revised: 9 April 2023

Accepted: 10 April 2023

Published: 15 April 2023



Copyright: © 2023 by the authors. Licensee MDPI, Basel, Switzerland. This article is an open access article distributed under the terms and conditions of the Creative Commons Attribution (CC BY) license (<https://creativecommons.org/licenses/by/4.0/>).

1. Introduction

OLEDs (organic light-emitting diodes) have gained widespread attention for their advantages such as low power consumption, high contrast, fast response time, thinner, and more foldable characteristics. According to the different driving methods, *OLED* driving technology can be divided into PMOLEDs (passive-matrix *OLEDs*) and AMOLED (active-matrix *OLEDs*). PMOLED has the advantages of a simple structure and low cost. However, PMOLED requires a larger driving voltage, and its power consumption is significantly higher than the AMOLED. As shown in Figure 1, AMOLEDs use independent thin-film transistors to control each pixel, so that each pixel can be continuously and independently driven and lit. Therefore, AMOLED is suitable for large and high-resolution displays, and has high application prospects for the displays [1–4].

In AMOLED pixel circuits, the oxide thin-film transistor (TFT) has great advantages, such as high carrier mobility, high light transmittance, good uniformity, and low off current, so it is widely applied to drive *OLED*, especially for large size AMOLED [5–9].

On the one hand, the TFT’s electrical characteristics variation, i.e., the threshold voltage variation and mobility variation would lead to the *OLED* current change. On the other hand, the *OLED* degradation would also lead to the *OLED* current change. The *OLED* current change brings out the uniformity of displays [10,11]. Therefore, in AMOLED displays, the circuit is needed to compensate the TFT’s electrical characteristics’ variation and the *OLED* degradation. Generally, the compensation circuit is divided into the current compensation circuit and the voltage compensation circuit.

The current compensation circuit can successfully compensate the TFT’s electrical characteristics’ variation [12,13]. However, the compensation speed is relatively slow at low gray level. This problem could be solved by the voltage compensation circuit [14–16].

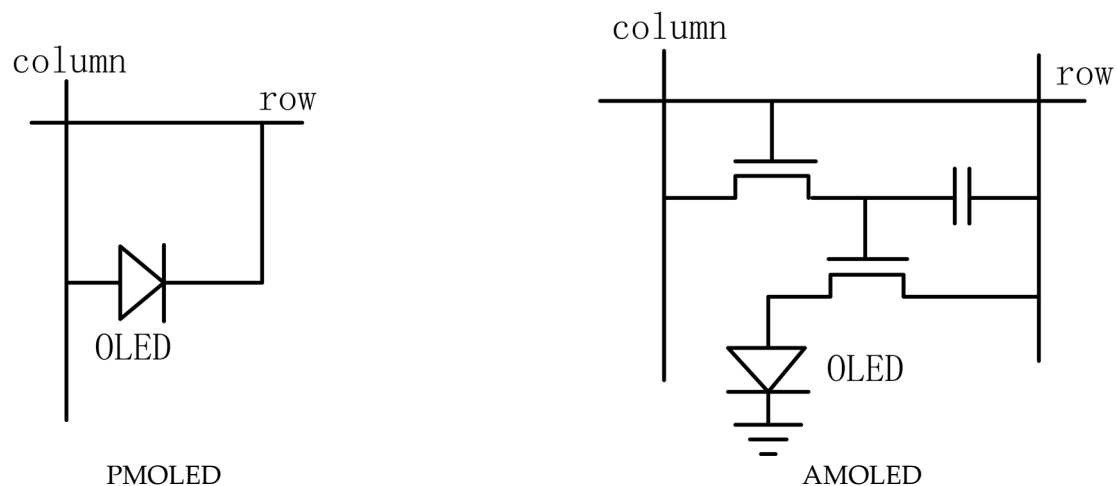


Figure 1. Schematic of PMOLED and AMOLED [4].

Therefore, lots of valuable voltage compensation pixel circuits have been reported [17–30].

In [17–21], the circuits can compensate the threshold voltage variation successfully. In [22–25], the circuits can compensate both threshold voltage and mobility variations successfully. In [26–28], the circuits can compensate both threshold voltage variation and *OLED* degradation successfully. To obtain higher uniformity of displays, it would be better if the circuits can compensate the above three items.

In [29], the circuit can compensate the above three items successfully, but the circuit cannot prevent the *OLED* flicker. In [30], the circuit not only can compensate the above three items, but also can prevent the *OLED* flicker successfully. However, the data voltage must be less than the *OLED* threshold voltage. Thus, the data voltage range is limited.

In this paper, a voltage compensation pixel circuit is proposed. In the threshold voltage extraction stage, the circuit can extract the threshold voltages of both the TFT and the *OLED* simultaneously. In the data input stage, the circuit can generate the mobility-related discharge voltage. The simulation results show that the circuit can compensate three items: the threshold voltage variation, the mobility variation, and the *OLED* degradation, can prevent the image flicker, and can achieve the wide data voltage range.

2. Materials and Methods

The circuit structure and the driving schematic diagram are shown in Figure 2. As shown in Figure 2a, the circuit consists of one driving TFT (T_2), four switching TFTs (T_1 , T_3 , T_4 , T_5), and two capacitors (C_1 , C_2).

As shown in Figure 2b, the driving schematic diagram contains four stages: (1) the initialization stage, (2) the threshold voltage extraction stage, (3) the data input stage, and (4) the emission stage.

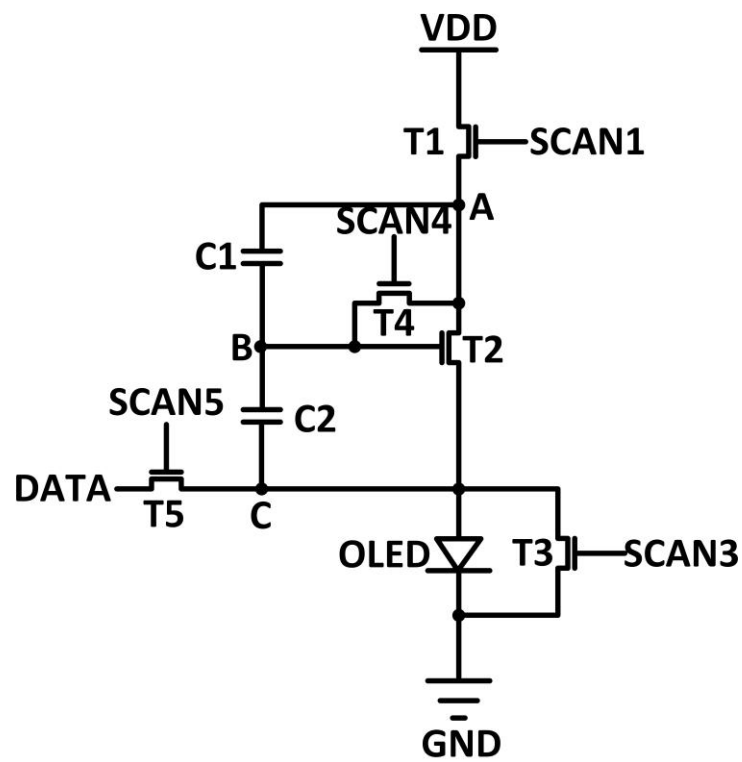
The working principle of the circuit is described as follows.

2.1. Initialization Stage

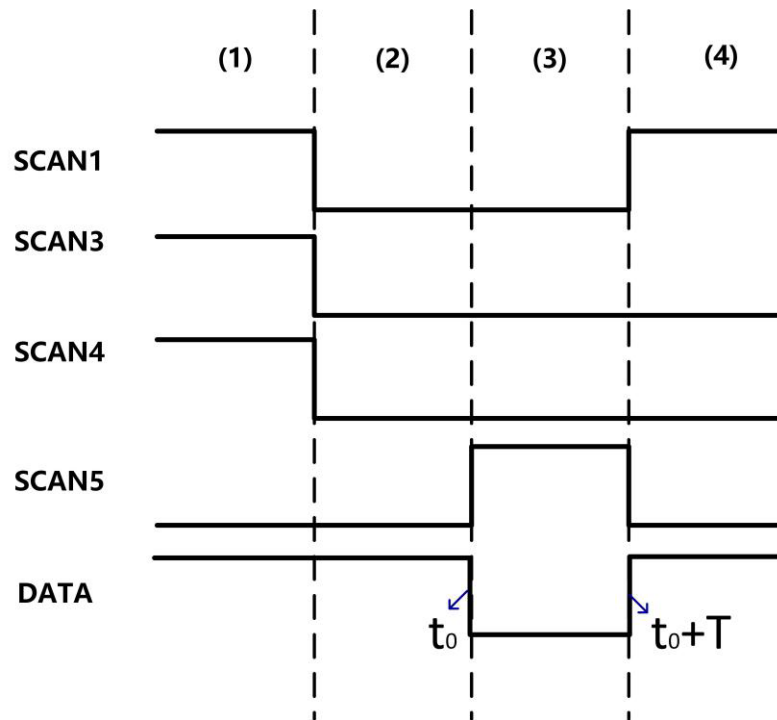
In the initialization stage, as shown in Figure 2b, SCAN1, SCAN3, and SCAN4 are high. SCAN5 is low. Therefore, T_1 , T_3 , and T_4 are turned on. T_5 is turned off. The schematic of the circuit in this stage is shown in Figure 3a.

Because T_1 and T_4 are turned on, the voltage of node B is charged to VDD.

Because T_3 is turned on, no current flows through the *OLED*. Therefore, the *OLED* flicker is prevented.



(a)



(b)

Figure 2. (a) Schematic of the proposed pixel circuit and (b) timing diagram: (1) initialization stage, (2) threshold voltage extraction stage, (3) data input stage, and (4) emission stage.

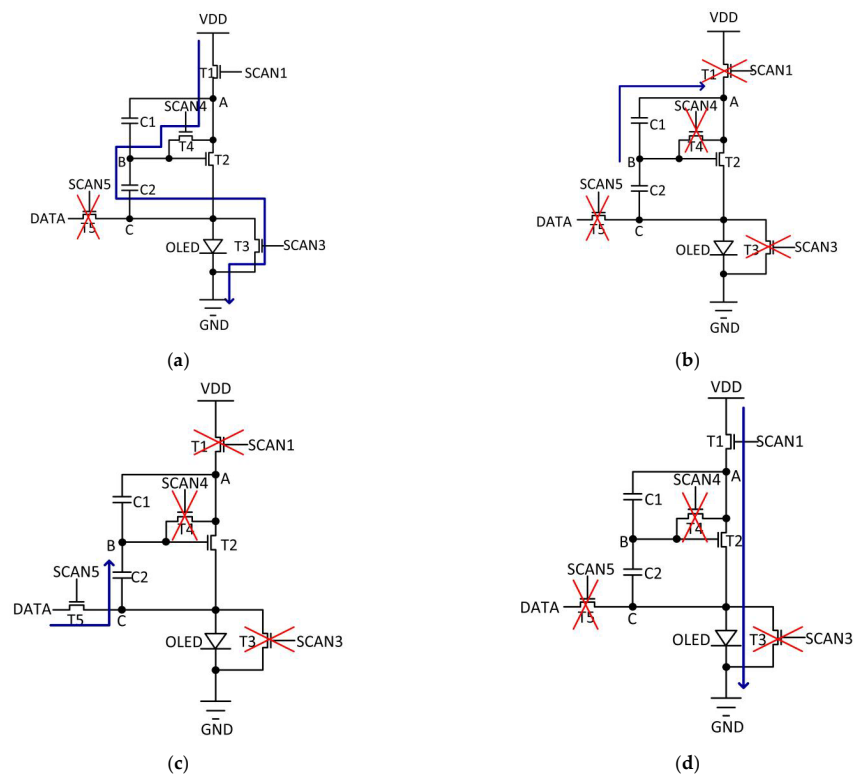


Figure 3. Schematic of the circuit operation in (a) initialization stage, (b) threshold voltage extraction stage, (c) data input stage, and (d) emission stage.

2.2. Threshold Voltage Extraction Stage

In the threshold voltage extraction stage, as shown in Figure 2b, SCAN1, SCAN3, and SCAN4 go to low. SCAN5 remains low. Therefore, $T1$, $T3$, $T4$, and $T5$ are turned off. The schematic of the circuit in this stage is shown in Figure 3b.

Because $T1$ is turned off, no current flows through the *OLED*. Therefore, the *OLED* flicker is prevented.

The voltage of node B is gradually discharged until $T2$ is turned off. The voltage of node B goes to

$$V_B = V_{TH_{T2}} + V_{TH_{OLED}}. \tag{1}$$

Consequently, the threshold voltages of both $T2$ and *OLED* are extracted simultaneously in this stage.

2.3. Data Input Stage

In the data input stage, as shown in Figure 2b, SCAN1, SCAN3 and SCAN4 remain low; SCAN5 goes to high. Therefore, $T1$, $T3$, and $T4$ are turned off; $T5$ is turned on. The schematic of the circuit in this stage is shown in Figure 3c.

Because $T1$ is turned off, no current flows through the *OLED*. Therefore, the *OLED* flicker is prevented.

In [29], to prevent *OLED* flicker, the data voltage range is limited: it is much less than the *OLED* threshold voltage. In this paper, the above limitation is avoided.

At the beginning and the end of this stage, t is defined as t_0 and $t_0 + T$, respectively. They are indicated in Figure 2b.

At the time t_0 , the data voltage (V_{DATA}) is input to the circuit; V_C and V_B are expressed as

$$V_C(t = t_0) = V_{DATA} + V_{TH_{OLED}}, \tag{2}$$

$$V_B(t = t_0) = V_{TH_{T2}} + V_{TH_{OLED}}. \tag{3}$$

After the time T , V_C remains unchanged; V_B discharges through $C1$, $C2$, and $T2$. At the time $t_0 + T$, V_C and V_B are expressed as

$$V_C(t = t_0) = V_{DATA} + V_{TH_OLED}, \quad (4)$$

$$V_B(t = t_0) = V_{TH_T2} + V_{TH_OLED} - (V_{DATA} + V_{TH_OLED}) \times \frac{C2}{C1 + C2} - \Delta V\mu. \quad (5)$$

where $\Delta V\mu$ is the discharged voltage related to the mobility of $T2$.

The expression of $\Delta V\mu$ is derived as follows. When $DATA$ is input to the circuit, $T2$ keeps the diode-connected structure. Therefore, the mobility-related discharge voltage $\Delta V\mu$ is stored in $C1$. By the law of discharge conservation, we have [30]

$$(C1 + C2) \frac{dV_{GS_T2}}{dt} = \frac{1}{2} \mu C_{OX} \frac{W}{L} (V_{GS_T2} - V_{TH_T2})^2. \quad (6)$$

where μ is the mobility of $T2$, C_{OX} is the gate oxide capacitance per unit area, and $\frac{W}{L}$ is the width-length ratio of $T2$.

Integrating (6), we have

$$\int_{V_{GS_T2}(t=t_0)}^{V_{GS_T2}(t=t_0+T)} \frac{1}{(V_{GS_T2} - V_{TH_T2})^2} dV_{GS_T2} = \int_{t=t_0}^{t=t_0+T} \frac{\mu C_{OX} \frac{W}{L}}{2(C1 + C2)} dt. \quad (7)$$

where

$$V_{GS_T2}(t = t_0) = V_B(t = t_0) - V_C(t = t_0), \quad (8)$$

$$V_{GS_T2}(t = t_0 + T) = V_B(t = t_0 + T) - V_C(t = t_0 + T). \quad (9)$$

Substituting (2)–(5) to (9), we obtain

$$\Delta V\mu = (V_{DATA} + V_{TH_OLED}) \times \frac{C2}{C1 + C2} - \frac{1}{\frac{\mu C_{OX} \frac{W}{L}}{2(C1 + C1)} T + \frac{1}{(V_{DATA} + V_{TH_OLED}) \times \frac{C2}{C1 + C2}}}. \quad (10)$$

Consequently, the mobility-related discharge voltage $\Delta V\mu$ is generated in this stage.

2.4. Emission Stage

In the emission stage, as shown in Figure 2b, SCAN1 goes to high, SCAN3 and SCAN4 remain low, and SCAN5 goes to low. Therefore, $T1$ is turned on, and $T3$, $T4$, and $T5$ are turned off.

The schematic of the circuit in this stage is shown in Figure 3d.

The driving TFT ($T2$) operates in the saturation region; the $OLED$ current is expressed as follows:

$$I_{OLED} = \frac{1}{2} \mu C_{OX} \frac{W}{L} (V_{GS_T2} - V_{TH_T2})^2. \quad (11)$$

Substituting (9) to (11), we obtain

$$I_{OLED} = \frac{1}{2} \mu C_{OX} \frac{W}{L} \left((V_{DATA} + V_{TH_OLED}) \times \frac{C2}{C1 + C2} - V_{DATA} - \Delta V\mu \right)^2. \quad (12)$$

Substituting (10) to (12), we obtain

$$I_{OLED} = \frac{1}{2} \mu C_{OX} \frac{W}{L} \left(\frac{1}{\frac{\mu C_{OX} \frac{W}{L}}{2(C1 + C1)} T + \frac{1}{(V_{DATA} + V_{TH_OLED}) \times \frac{C2}{C1 + C2}}} - V_{DATA} \right)^2. \quad (13)$$

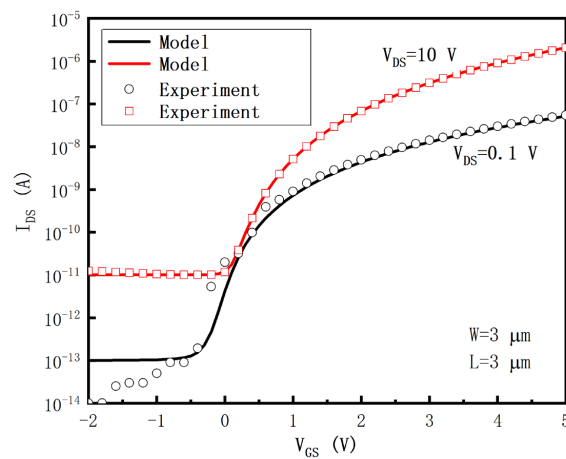
From (12), it is found that the OLED current is independent of the threshold voltage V_{TH_T2} . That is, when V_{TH_T2} varies, I_{OLED} remains stable. Therefore, the circuit can compensate the threshold voltage variation.

From (10), it is found that when the mobility μ increases, $\Delta V\mu$ will increase, and vice versa. Consequently, in (12), when the mobility varies, I_{OLED} remains stable. Therefore, the circuit can compensate the mobility variation. This point also can be explained by (13). In (13), when μ increases, both $\frac{1}{2}\mu C_{OX} \frac{W}{L}$ and $\frac{\mu C_{OX} \frac{W}{L}}{2(C_1+C_2)} T$ will increase; thus, I_{OLED} remains stable, and vice versa.

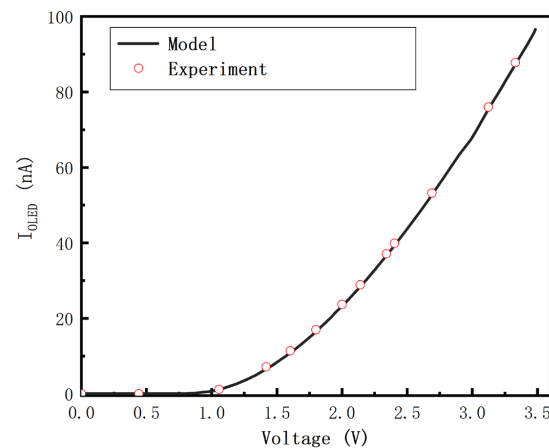
From (13), it is found that the OLED current is positively correlated with V_{TH_OLED} . Therefore, the circuit can compensate the OLED degradation [29–31].

3. Results and Discussions

In the circuit simulation, to evaluate the compensation performance, the SPICE model (level = 35) is used for the oxide TFTs. The TFTs' threshold voltage and mobility are 1.5 V and $50 \text{ cm}^2/\text{V}$, respectively. The TFTs' threshold voltage variation and mobility variation are $\pm 0.5 \text{ V}$ and $\pm 30\%$, respectively [9,14,28]. The OLED model is equivalent to a TFT and a C_{OLED} in parallel [22,27,32]. The oxide TFT and the OLED models are verified by the experimental data [8,33], which are shown in Figure 4.



(a)



(b)

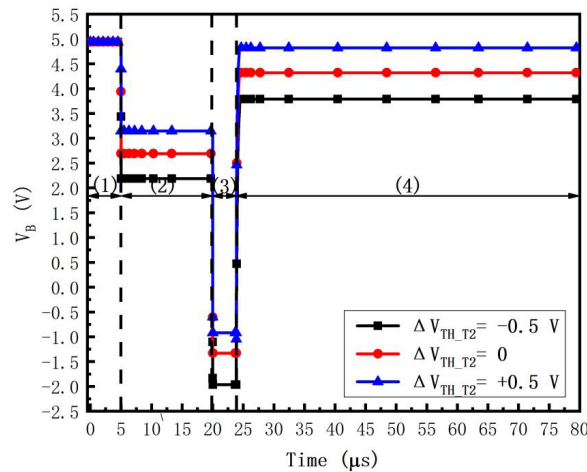
Figure 4. (a) The transfer characteristic of the a-IGZO TFT [8], and (b) the electrical characteristic of the OLED [33].

The values of the design parameters are shown in Table 1; the range of the values is reasonable, which is consistent with the previous pixel circuit applications [11,19,20,27,32,34].

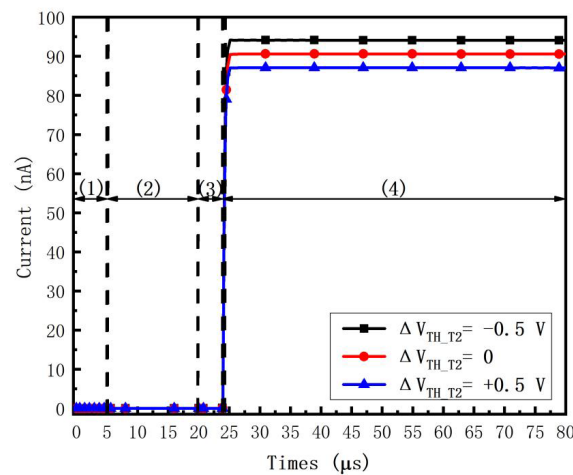
Table 1. Design parameters of the circuit.

Parameters (Unit)	Value	Parameters (Unit)	Value
W_{T2} (μm)	3	VDD (V)	5
L_{T2} (μm)	3	C2 (pF)	0.2
$W_{T1,T3,T4,T5}$ (μm)	22	C_{OLED} (pF)	0.2
$L_{T1,T3,T4,T5}$ (μm)	3	SCAN _{1,3,4,5} (V)	-5~5
C1 (pF)	0.4	DATA (V)	$V_{DATA} \sim 0$

Figure 5a shows the transient waveforms of V_B , i.e., the gate voltage of T2, at $V_{DATA} = -4$ V. It is found that when $\Delta V_{TH_T2} = \pm 0.5$ V, ΔV_B approximates ± 0.5 V in the threshold voltage extraction stage, i.e., V_B senses the threshold voltage variation successfully. Figure 5b shows the transient waveforms of the OLED current I_{OLED} . It is found that $I_{OLED} = 0$ except for the emission stage, i.e., the OLED flicker is prevented. In the emission stage, when $\Delta V_{TH_T2} = -0.5, 0,$ and $+0.5$ V, the transient waveforms of $I_{OLED} = 94.11, 90.59,$ and 87.06 nA, respectively. The current error rates (CERs) are 3.74% and 0, 3.89%, respectively. Thus, the circuit compensates ΔV_{TH_T2} successfully.

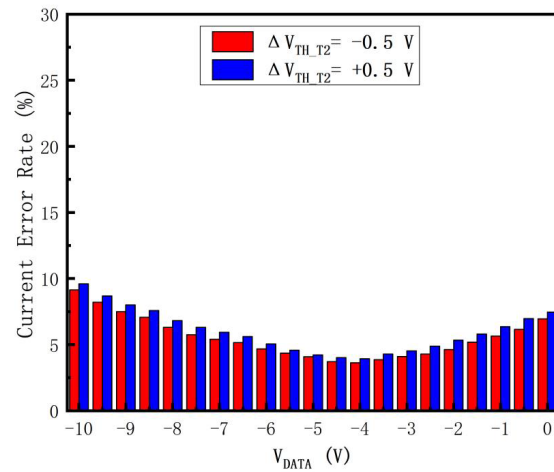


(a)



(b)

Figure 5. Cont.



(c)

Figure 5. Transient waveforms of (a) V_B and (b) I_{OLED} when $\Delta V_{TH_T2} = -0.5, 0,$ and $+0.5$ V at $V_{DATA} = -4$ V, where (1) initialization stage, (2) threshold voltage extraction stage, (3) data input stage, (4) emission stage, and (c) current error rates versus V_{DATA} when the threshold voltage varies.

The CER for ΔV_{TH_T2} is defined as

$$\frac{I_{OLED}(\Delta V_{TH_T2} = 0) - I_{OLED}(\Delta V_{TH_T2} = \pm 0.5 \text{ V})}{I_{OLED}(\Delta V_{TH_T2} = 0)} \times 100\%. \quad (14)$$

Figure 5c shows the transient waveforms of CER vary when ΔV_{TH_T2} is $+0.5$ V and -0.5 V, respectively. It is found that the CERs are less than $\pm 9.59\%$ within the whole data range. Thus, the threshold voltage variation ΔV_{TH_T2} is compensated successfully.

Figure 6a shows the transient waveforms of V_B at $V_{DATA} = -4$ V. It is found that when $\Delta u = \pm 30\%$, the variation of V_B is similar to Δu , i.e., V_B senses the mobility variation successfully. Figure 6b shows the transient waveforms of the OLED current I_{OLED} . It is found that $I_{OLED} = 0$ except for the emission stage, i.e., the OLED flicker is prevented. In the emission stage, when $\Delta u = -30, 0,$ and $+30\%$, the transient waveforms of $I_{OLED} = 88.06, 90.59,$ and 93.87 n A, respectively. The current error rates are 2.81% and $0, 3.49\%$, respectively. Thus, the circuit compensates Δu successfully.

The CER for Δu is defined as

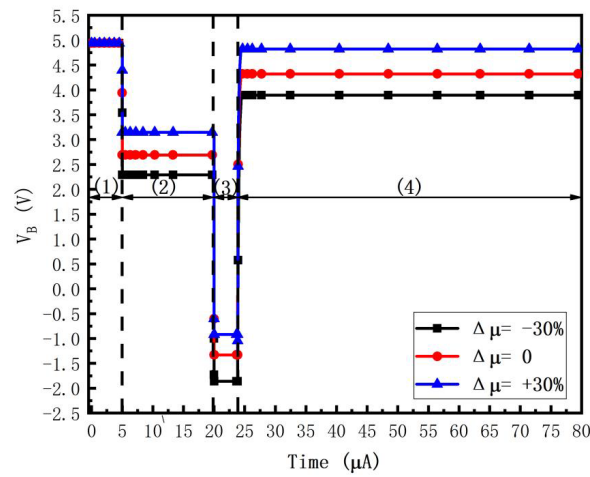
$$\frac{I_{OLED}(\Delta u = 0) - I_{OLED}(\Delta u = \pm 30\%) }{I_{OLED}(\Delta u = 0)} \times 100\%. \quad (15)$$

Figure 6c shows the transient waveforms of CER varies when Δu is $+30\%$ and -30% , respectively. It is found that the CERs are less than $\pm 9.28\%$ within the whole data range. Thus, the mobility variation Δu is compensated successfully.

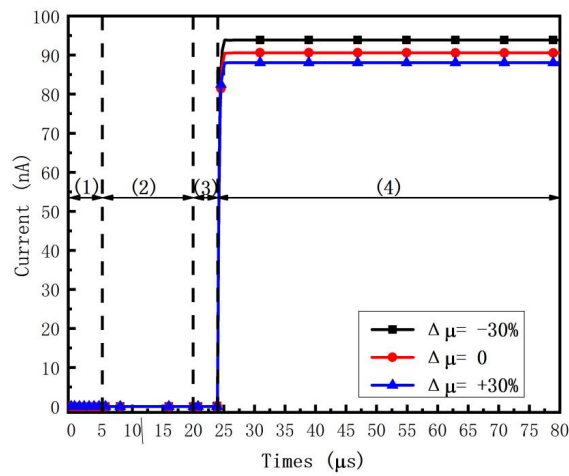
In this paper, the circuit can compensate the OLED degradation. It is explained as follows. For the long time operation, the OLED luminance degrades while V_{TH_OLED} increases [29–31]. Therefore, I_{OLED} (13) increases. The increase in I_{OLED} brings about the increase in the OLED luminance. Thus, the OLED luminance degradation is compensated.

In Figures 5a,b and 6a,b, the time of the third stage, i.e., the data input stage, is set to 3.8 μ s. It is suitable for the 8K4K ultrahigh definition (7680×4320 , UHD) for high-performance display [11,35,36].

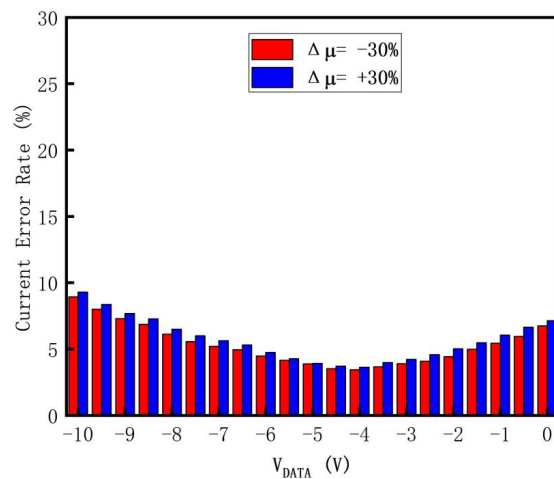
As shown in Table 2, the valuable publications are compared with this paper. In [29], the circuit can compensate the threshold voltage variation, the mobility variation, and the OLED degradation successfully, but the circuit cannot prevent the OLED flicker. In [30] and this paper, the circuits not only can compensate the above three items successfully, but also can prevent the OLED flicker.



(a)



(b)



(c)

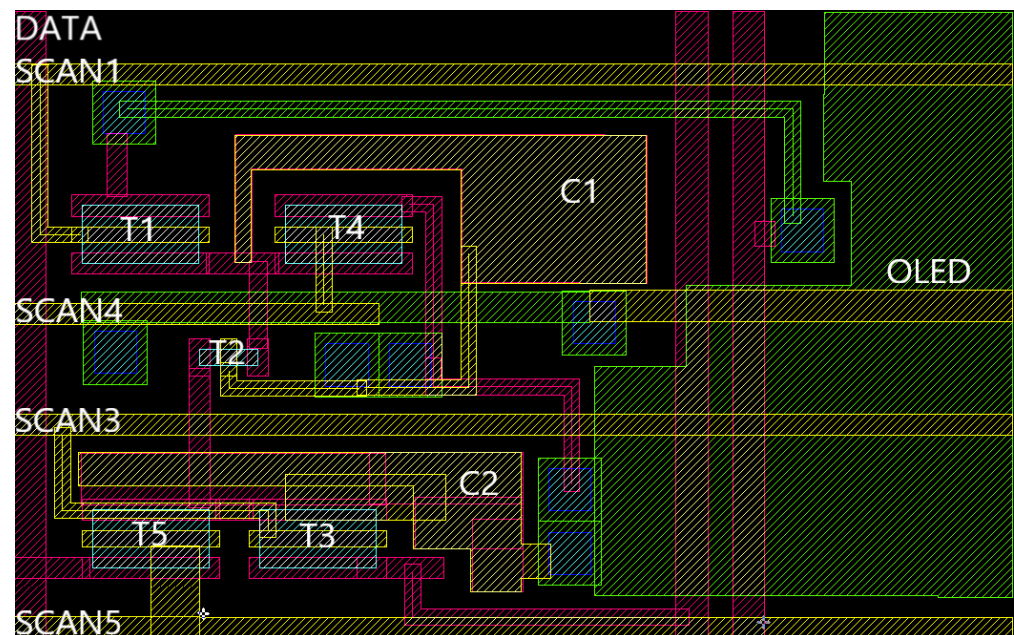
Figure 6. Transient waveforms of (a) V_B and (b) I_{OLED} when $\Delta\mu = +30\%$, 0 , and -30% at $V_{DATA} = -4V$, where (1) initialization stage, (2) threshold voltage extraction stage, (3) data input stage, (4) emission stage, and (c) current error rates versus V_{DATA} when the threshold voltage varies.

Table 2. Comparison between this paper and the previous publications.

Publications	Structure	V_{TH} Compensation	μ Compensation	OLED Degradation	Prevent Image Flicker
2015 [22]	5T2C	✓	✓	-	✓
2015 [27]	5T2C	✓	-	✓	✓
2015 [28]	4T1C	✓	-	✓	✓
2016 [30]	4T2C	✓	✓	✓	✓
2017 [26]	4T1C	✓	-	✓	✓
2018 [23]	6T2C	✓	✓	-	✓
2018 [29]	5T2C	✓	✓	✓	-
2020 [19]	6T1C	✓	-	-	✓
2020 [20]	9T2C	✓	-	-	✓
2022 [17]	6T2C	✓	-	-	✓
This paper	5T2C	✓	✓	✓	✓

However, in [30], V_{DATA} must be less than V_{TH_OLED} , that is, the range of V_{DATA} is limited. In this paper, the range of V_{DATA} is not limited by V_{TH_OLED} . Therefore, the circuit achieves the wide data voltage range.

Figure 7 shows the layout structure of the circuit. SCAN1, SCAN3, SCAN4, and SCAN5 are transverse lines, which are set to 4 μm . These transverse lines are shared by the pixels of the same row. VDD, GND, and DATA are the vertical lines, which are set to 6 μm . VDD and GND are shared by the entire display panel. DATA is shared by the pixels of the same column. The total layout area is 180 $\mu\text{m} \times 110 \mu\text{m}$. The proposed layout achieves an aperture ratio of 39.14%.

**Figure 7.** Layout structure of the circuit.

4. Conclusions

The pixel circuit is presented for improving AMOLED displays uniformity. In the threshold voltage extraction stage, the threshold voltages of the driving TFT and the OLED are extracted. In the data input stage, the discharge voltage related to mobility is generated. Consequently, the circuit not only compensates the threshold voltage variation, the mobility variation, and the OLED degradation, but also prevents the image flicker and achieves the wide data voltage range.

Author Contributions: N.W.: Conceptualization, Methodology, Validation, Formal Analysis, Investigation, Writing—Original Draft; H.C.: Investigation; B.Y.: Investigation; H.Z.: Investigation; Y.L.: Supervision, Writing—Review & Editing; X.W.: Project Administration, Funding Acquisition; H.H.: Supervision, Writing—Review & Editing. All authors have read and agreed to the published version of the manuscript.

Funding: This research was funded by [The Hunan Province Key Laboratory for Ultra-Fast Micro/Nano Technology and Advanced Laser Manufacture] grant number [No. 2018TP1041].

Data Availability Statement: Data sharing is not applicable to this article as no new data were created or analyzed in this study.

Conflicts of Interest: The authors declare no conflict of interest.

References

1. Singh, A.; Goswami, M.; Kandpal, K. Design of a voltage-programmed V_{TH} compensating pixel circuit for AMOLED displays using diode-connected a-IGZO TFT. *IET Circuits Devices Syst.* **2020**, *14*, 876–880. [\[CrossRef\]](#)
2. Srivastava, A.; Dubey, D.; Goswami, M.; Kandpal, K. Mechanical strain and bias-stress compensated, 6T-1C pixel circuit for flexible AMOLED displays. *Microelectron. J.* **2021**, *117*, 105266. [\[CrossRef\]](#)
3. Zhao, B.; Xiao, J.; Liu, Q.; Liu, B.; Hu, L.; Peng, J. A novel compensation pixel circuit for high bits of AM mini/micro-LED based on PWM method. *Energy Rep.* **2021**, *7*, 343–348. [\[CrossRef\]](#)
4. Lin, C.-L.; Chang, W.-Y.; Hung, C.-C.; Tu, C.-D. LTPS-TFT pixel circuit to compensate for OLED luminance degradation in three-dimensional AMOLED display. *IEEE Electron Device Lett.* **2012**, *33*, 700–702. [\[CrossRef\]](#)
5. Lee, J.S.; Chang, S.; Koo, S.-M.; Lee, S.Y. High-performance a-IGZO TFT with ZrO_2 gate dielectric fabricated at room temperature. *IEEE Electron Device Lett.* **2010**, *31*, 225–227. [\[CrossRef\]](#)
6. Yao, J.; Xu, N.; Deng, S.; Chen, J.; She, J.; Liu, P.; Huang, Y. Electrical and photosensitive characteristics of a-IGZO TFTs related to oxygen vacancy. *IEEE Trans. Electron Devices* **2011**, *58*, 1121–1126. [\[CrossRef\]](#)
7. Hong, S.-K.; Kim, B.-K.; Ha, Y.-M. LTPS technology for improving the uniformity of AMOLEDs. *SID Symp. Dig.* **2007**, *38*, 1366–1369. [\[CrossRef\]](#)
8. Liao, C. Mobility impact on compensation performance of AMOLED pixel circuit using IGZO TFTs. *J. Semicond.* **2019**, *40*, 022403. [\[CrossRef\]](#)
9. Lin, C.-L.; Chen, F.-H.; Liu, Y.-T.; Lu, C.-M.; Wu, W.-L. New voltage-programmed AMOLED pixel circuit employing in-pixel compensation scheme for mobility variation. *SID Symp. Dig.* **2016**, *47*, 1254–1256. [\[CrossRef\]](#)
10. Lin, Y.-C.; Shieh, H.-P.D.; Kanicki, J. A novel current-scaling a-Si: H TFTs pixel electrode circuit for AM-OLEDs. *IEEE Trans. Electron Devices* **2005**, *52*, 1123–1131. [\[CrossRef\]](#)
11. Lai, P.-C.; Lin, C.-L.; Kanicki, J. Novel top-anode OLED/a-IGZO TFTs pixel circuit for 8K4K AM-OLEDs. *IEEE Trans. Electron Devices* **2018**, *66*, 436–444. [\[CrossRef\]](#)
12. Pappas, I.; Voudouris, L.; Tarawneh, B.K.; Rjoub, A.; Nikolaidis, S. A new current-programmed pixel design for AMOLED displays implemented with organic thin-film transistors. In Proceedings of the 2012 28th International Conference on Microelectronics Proceedings, Nis, Serbia, 13–16 May 2012; pp. 77–80. [\[CrossRef\]](#)
13. Lee, J.-H.; Nam, W.-J.; Jung, S.-H.; Han, M.-K. A New Current Scaling Pixel Circuit for AMOLED. *IEEE Electron Device Lett.* **2004**, *25*, 280–282. [\[CrossRef\]](#)
14. Zeng, Y.; Chu, H.; Wei, N.; Li, Y.; Wang, X.; He, H. A 5T1C pixel circuit compensating mobility and threshold voltage variation. *Microelectron. J.* **2021**, *117*, 105283. [\[CrossRef\]](#)
15. Chen, C.; Abe, K.; Kumomi, H.; Kanicki, J. a-InGaZnO thin-film transistors for AMOLEDs: Electrical stability and pixel-circuit simulation. *J. Soc. Inf. Disp.* **2009**, *17*, 525–534. [\[CrossRef\]](#)
16. Shin, W.-S.; Ahn, H.-A.; Na, J.-S.; Hong, S.-K.; Kwon, O.-K.; Lee, J.-H.; Um, J.-G.; Jang, J.; Kim, S.-H.; Lee, J.-S. A driving method of pixel circuit using a-IGZO TFT for suppression of threshold voltage shift in AMOLED displays. *IEEE Electron Device Lett.* **2017**, *38*, 760–762. [\[CrossRef\]](#)
17. Pal, S.; Kumar, B. Threshold voltage compensation 6T2C-pixel circuit design using OTFT for flexible display. *Microelectron. J.* **2020**, *102*, 104818. [\[CrossRef\]](#)
18. Fan, C.-L.; Chen, C.-Y.; Tseng, F.-P.; Yang, C.-C.; Chien, K.-E.; Hsiao, Y.-H. 3T0.5C Compensating pixel circuit with all p-type LTPS-TFTs for AMOLED displays. *Displays* **2018**, *53*, 8–13. [\[CrossRef\]](#)
19. Ke, J.; Deng, L.; Zhen, L.; Wu, Q.; Liao, C.; Luo, H.; Huang, S. An AMOLED pixel circuit based on LTPS thin-film transistors with mono-type scanning driving. *Electronics* **2020**, *9*, 574. [\[CrossRef\]](#)
20. Lin, C.-L.; Chang, J.-H.; Lai, P.-C.; Shih, L.-W.; Chen, S.-C.; Cheng, M.-H. Pixel circuit with leakage prevention scheme for low-frame-rate AMOLED displays. *IEEE J. Electron Devices Soc.* **2020**, *8*, 235–240. [\[CrossRef\]](#)
21. Fan, C.-L.; Tsao, H.-Y.; Chen, C.-Y.; Chou, P.-C.; Lin, W.-Y. New low-voltage driving compensating pixel circuit based on high-mobility amorphous indium-zinc-tin-oxide thin-film transistors for high-resolution portable active-matrix OLED displays. *Coatings* **2020**, *10*, 1004. [\[CrossRef\]](#)

22. Lin, C.-L.; Lai, P.-C.; Deng, M.-Y. P-43: New pixel circuit to improve current uniformity for high-resolution AMOLED displays. *SID Symp. Dig. Tech. Pap.* **2015**, *46*, 1297–1300. [[CrossRef](#)]
23. Wu, J.; Yi, S.; Liao, C.; Huo, X.; Wang, Y.; Zhang, S. New AMOLED pixel circuit to compensate characteristics variations of LTPS TFTs and voltage drop. In Proceedings of the 2018 25th International Workshop on Active-Matrix Flatpanel Displays and Devices (AM-FPD), Kyoto, Japan, 3–6 July 2018. [[CrossRef](#)]
24. Liao, C.; Deng, W.; Song, D.; Huang, S.; Deng, L. Mirrored OLED pixel circuit for threshold voltage and mobility compensation with IGZO TFTs. *Microelectron. J.* **2015**, *46*, 923–927. [[CrossRef](#)]
25. Ho, C.-H.; Lu, C.; Roy, K. An enhanced voltage programming pixel circuit for compensating GB-induced variations in poly-Si TFTs for AMOLED displays. *J. Disp. Technol.* **2014**, *10*, 345–351. [[CrossRef](#)]
26. Kim, D.; Kim, Y.; Lee, S.; Kang, M.S.; Kim, D.H.; Lee, H. High resolution a-IGZO TFT pixel circuit for compensating threshold voltage shifts and OLED degradations. *IEEE Trans. Electron Devices* **2017**, *5*, 372–377. [[CrossRef](#)]
27. Lin, C.-L.; Liu, Y.-T.; Lee, C.-E.; Chen, P.-S.; Chu, T.-C.; Hung, C.-C. a-InGaZnO active-matrix organic LED pixel periodically detecting thin-film transistor threshold voltage once for multiple frames. *IEEE Electron Device Lett.* **2015**, *36*, 1166–1168. [[CrossRef](#)]
28. Wang, C.; Leng, C.; Wang, L.; Lu, W.; Zhang, S. An accurate and fast current-biased voltage-programmed AMOLED pixel circuit with OLED biased in AC mode. *J. Disp. Technol.* **2015**, *11*, 615–619. [[CrossRef](#)]
29. Yi, S.; Huo, X.; Liao, C.; Wang, Y.; Wu, J.; Jiao, H.; Zhang, M.; Zhang, S. An a-IGZO TFT pixel circuit for AMOLED display systems with compensation for mobility and threshold voltage variations. In Proceedings of the 2018 IEEE International Conference on Electron Devices and Solid State Circuits (EDSSC), Shenzhen, China, 6–8 June 2018. [[CrossRef](#)]
30. Lin, C.-L.; Lai, P.-C.; Chen, P.-C.; Wu, W.-L. Pixel circuit with parallel driving scheme for compensating luminance variation based on a-IGZO TFT for AMOLED displays. *J. Disp. Technol.* **2016**, *12*, 1681–1687. [[CrossRef](#)]
31. Lin, C.-L.; Chen, Y.-C. A novel LTPS-TFT pixel circuit compensating for TFT threshold-voltage shift and OLED degradation for AMOLED. *IEEE Electron Device Lett.* **2007**, *28*, 129–131. [[CrossRef](#)]
32. Lin, C.-L.; Lai, P.-C.; Chan, J.-H.; Chen, S.-C.; Tsai, C.-L.; Koa, J.-L.; Cheng, M.-H.; Shih, L.-W.; Hsu, W.-C. Leakage-Prevention mechanism to maintain driving capability of compensation pixel circuit for low frame rate AMOLED displays. *IEEE Trans. Electron Devices* **2021**, *68*, 2313–2319. [[CrossRef](#)]
33. Huo, X.; Liao, C.; Zhang, M.; Jiao, H.; Zhang, S. A pixel circuit with wide data voltage range for OLEDs microdisplays with high uniformity. *IEEE Trans. Electron Devices* **2019**, *66*, 4798–4804. [[CrossRef](#)]
34. Chang, J.-H.; Shih, L.-W.; Lin, C.-L. New pixel circuit with negative feedback scheme for AMOLED smartwatch displays. In Proceedings of the 2021 28th International Workshop on Active-Matrix Flatpanel Displays and Devices (AM-FPD), Kyoto, Japan, 29 June–2 July 2021; pp. 129–132. [[CrossRef](#)]
35. Hara, Y.; Kikuchi, T.; Kitagawa, H.; Morinaga, J.; Ohgami, H.; Imai, H.; Daitoh, T.; Matsuo, T. IGZO-TFT technology for large-screen 8K display. *SID Symp. Dig.* **2018**, *26*, 169–177. [[CrossRef](#)]
36. Yamamoto, R.; Kobayashi, H.; Takahashi, K.; Isaka, F.; Hirakata, Y.; Bergquist, J.; Yamazaki, S.; Dobashi, M.; Kokubo, R.; Ono, K. 7-1: Distinguished Paper: 13.3-inch 8k4k 664-ppi 120-Hz 12-bit OLED display using top-gate self-align CAAC-OS FETs and 12-bit source driver IC. *SID Symp. Dig.* **2016**, *47*, 53–56. [[CrossRef](#)]

Disclaimer/Publisher’s Note: The statements, opinions and data contained in all publications are solely those of the individual author(s) and contributor(s) and not of MDPI and/or the editor(s). MDPI and/or the editor(s) disclaim responsibility for any injury to people or property resulting from any ideas, methods, instructions or products referred to in the content.